Materials Science for Energy Technologies 3 (2020) 282–288

Contents lists available at ScienceDirect

Materials Science for Energy Technologies

journal homepage: www.keaipublishing.com/en/journals/materials-science-for-energy-technologies

Physico-chemical, structural, optical and NLO studies on pure and La^{3+} doped L-arginine acetate crystals

A. Senthamizhan [a], K. Sambathkumar [b], S. Nithiyanantham [c,*]

[a] V.R.S. College of Engineering and Technology, Villupuran, Tamil Nadu 605602, India
[b] PG & Research Department of Physics, A.A. Govt. Arts College, Villupuram 605602, India
[c] PG & Research Department of Physics, Thiru. Vi. Ka. Govt Arts and Science College, Thiruvarur, Tamil Nadu 610003, India

ARTICLE INFO

Article history:
Received 20 May 2019
Revised 13 November 2019
Accepted 22 November 2019
Available online 11 December 2019

Keywords:
L-Arginine acetate
FT-IR
FT-Raman
UV–Vis-NIR
Thermal and microhardness
Dielectric

ABSTRACT

Pure and La^{3+} doped single crystals of L-arginine acetate (LAA) have been grown well from through slow evaporation method in aqueous environment. The Crystalline nature can be confirmed by powder X-Ray Diffraction (XRD) Analysis. The function groups with possible stretching/bonding were identified through FTIR (Fourier Transform Infrared Spectroscopy) and Fourier Transform Raman Spectroscopy (FT-Raman) analysis. The good optical properties of La^{3+} doped LAA crystals were found through UV–Visible spectral analysis. Nonlinear optical (NLO) behavior through Kurtz's method reveals that the dopant has increased the efficiency. Further, grown crystals has examined for thermal (TGA, DTA), mechanical (Vicker's), dielectric (LCR) and photo conductive (picoammeter) properties enhanced with La^{3+} dopant and the results are interpreted and discussed.

1. Introduction

In recent times, the non-linear optical (NLO) materials having attracting the attention towards to formation of active and functional devices. The organic NLO materials with higher harmonic generation properties leads to the new development in modern engineering optic and semiconducting, photonic and optoelectronic devices, etc., used in opto-electronic, photonic and many areas because of the property of optical second harmonic generation (SHG) [1–4]. Mostly amino acids having SHG properties due to their chiral carbon with non-centro symmetric nature. Present day Arginine crystal attracts much attention towards the optical, thermal, mechanical, dielectric behavior and etc., and better choice for device applications [5–8], in polyhedron (1 0 0) face [9,10]. The LAA was found higher SHG efficiency than that of KDP [11]. The optical materials which exhibit centrosymmetric behavior exhibit NLO and ferroelectric property [12].

The molecular hyperpolarizability (β) is the backbone of second harmonic generation response. In general, organic molecules exhibit large β values rather than inorganic molecules and suitable for photoconductive property [13–16]. Amino acids contain a proton donor carbon carbonyl acid (COO^-) group and the proton acceptor (NH_2^+) itself [17–20].

And there is a need of ferroelectric materials having nonvolatile memory and so the scientific society demanding materials dual nature of modern with ferroelectric and piezoelectric properties. Optical materials with rare earth dopant such as La3+, Cu2+, Mg2 + and etc, are enhancing the Photoconductive properties [21–23].

The present investigation deals with the formation of LAA and La^{3+}metal doped LAA crystals through evaporation method. The content of the dopant was determined by Inductively Coupled Plasma analysis. The grown crystals are investigated with many spectroscopic techniques and are presented the following section 2. The findings and results of these investigations are interpreted and discussed in Section 3 and 4.

2. Synthesis and solubility

The AR grades chemical were purchased from S.D. Fine chemicals, India. The synthesis of LAA through the standard procedure [9].

The pure LAA is synthesized and the product was allowed to evaporate and collected as salt. The LAA with metal dopant La^{3+} of 2 mol % is added with same procedure. The solubility of both

* Corresponding author.
E-mail addresses: s_nithu59@rediffmail.com, prof.nithiyanantham.s@tvkgovac.in (S. Nithiyanantham).

Peer review under responsibility of KeAi Communications Co., Ltd.

https://doi.org/10.1016/j.mset.2019.11.005

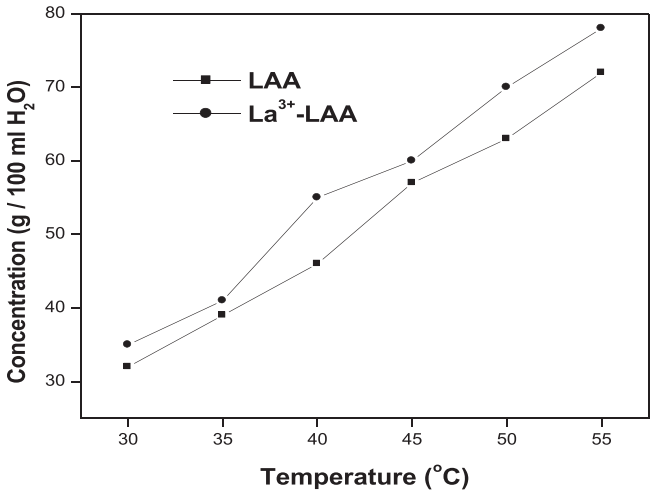

Fig. 1. Solubility (a) LAA, (b) La^{3+} doped LAA crystal.

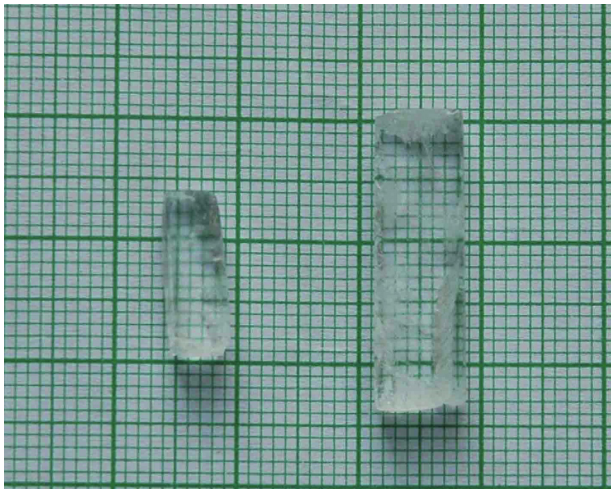

Fig. 2. LAA and La^{3+} doped LAA crystal.

pure and doped LAA was measured at various temperatures from 30 to 55 in steps of 5 °C with an accuracy of ±0.01 °C. Fig. 1, plots of temperature vs concentration shows that the solubility is always increases with temperature for both samples. The dopant La^{3+} added in the parent solution as prepared in pure form and the grown crystals free from defect is shown in Fig. 2.

3. Characterization

The Powder XRD analysis of both crystals are carried out through Rich Seifert, XRD 3000P with Cu Kα (λ = 1.54056 Å) radiation. Wt. percentage of samples studied through inductively coupled plasma (ICP) analysis. The FTIR spectra are recorded using MAGNA 550 model spectrometer. The stretching and function groups, chemical nature carried out through FTIR and FT-Raman spectral analysis. The thermo-gravimetric analyses performed through STA 409C set up with temperature from 23 to 1200 °C under nitrogen environment. The micro-hardness study carried out through Vickers's hardness test. The SHG analysis carried out through Nd:YAaG laser with an input pulse of 6.2 mJ. The dielectric analysis carried out through LCR meter. The photoconductive measurements carried out through Keithley 485 picoammeter [30].

4. Results and discussion

4.1. Powder XRD studies

The XRD patterns of grown samples of pure and La^{3+} doped LAA were depicted in Fig. 3. The lattice constant were presented in the Table.1, The lattice parameters indicate that both type of crystals in monoclinic with $P2_1$ space group and these are well agreed with standard values [9,11]. Slight variations observed in both crystals and so the presence of dopant causes small changes in their properties.

4.2. Inductively coupled plasma analysis

The weight percentage of La^{3+} doped LAA crystal about 10 mg in 100 ml distilled water. Further the samples were subjected to Inductive coupled plasma (ICP) analysis, the results shows 1.03% of La^{3+} existed in the solution. It confirmed that the presence of the amount of La3+ metal ion dopant is less than 2%.

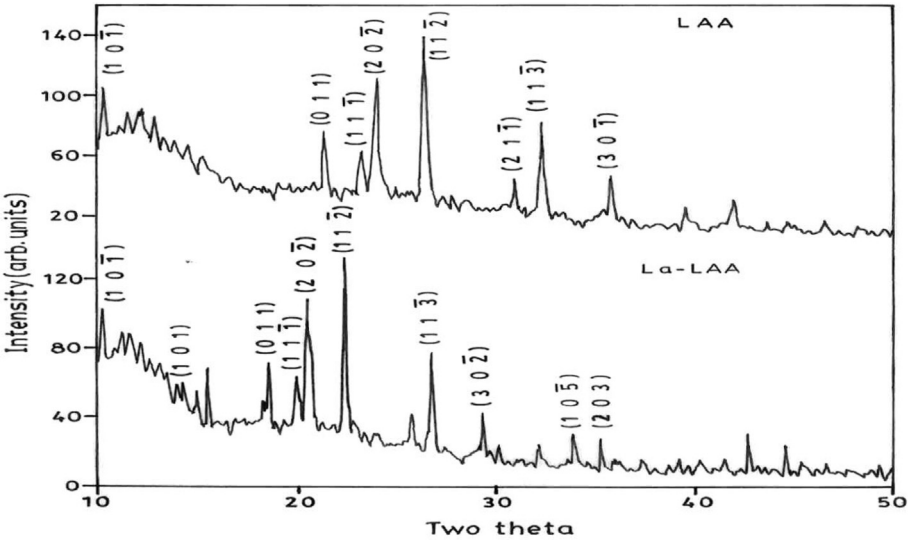

Fig. 3. Powder XRD pattern LAA, La3+ doped LAA crystal.

Table 1
Lattice parameters for pure and La^{3+} doped LAA crystal.

Lattice parameters	LAA	La^{3+} + LAA	LAA [11,13]
a (Å)	9.209	9.122	9.220
b (Å)	5.201	5.252	5.185
c (Å)	13.101	12.801	13.100
α(°)	90	90	90
β(°)	108.91	107.54	109.6
γ(°)	90	90	90
Crystal System	Monoclinic	Monoclinic	Monoclinic
Space group	$P2_1$	$P2_1$	$P2_1$
Volume (Å^3)	586.20	581.38	587

Table 2
FT-IR spectral assignments of LAA, and LAA + La^{3+} Crystal.

Wave number (cm^{-1})	Assignments	
Pure LAA	La^{3+}-LAA	
3750–2300	3750–2300	NH and CH stretching vibration
1532	1531	COO^- asymmetric stretching
1400	1400	COO^- symmetric stretching
1228, 1197	1229, 1196	COO^- vibration
1093	1089	C-N stretching
928	929	CH_2 rocking
890	891	C–C stretching [3]
670	669	NH_2 out of plane

4.3. FT-IR analysis

The middle infrared spectra of pure and doped L-arginine acetate are shown in Fig. 4. Both doped and pure crystals shows absorption at 1620 cm^{-1} shows the existence of presence of amino group, the absorption at 1550 cm^{-1} show cyclic –NH stretching and O–H stretching. The FT-IR Spectra LAA confirms the structural aspects.

In addition, there is not much difference are observed in the presence of dopant. The percentage changes of transmittance are worth noting. More absorption near 3000 cm^{-1} indicates the presence of both C=O stretching and O–H stretching. The IR spectrum indicates that the absence of water and there is no existence of OH stretching at 3400 cm^{-1} (Table 2) [21,24].

4.4. FT-Raman spectra

The FT-Raman spectra of LAA and LAA+ La^{3+} crystals are shown in Fig. 5. The observed peaks confirm the existence of dopant in the LAA crystal. The N–H stretching found at, and from 3100 cm^{-1} to 2600 cm^{-1} form a wide strong bond with many peaks. The band at 1579 cm^{-1} is indicating asymmetric N–H deformation. The absorption at 3065 cm^{-1} indicates N–H stretching by amino group. The spectra further shows the peaks at 1415 cm^{-1} and 1626 cm^{-1} are due to the C=O stretching of carboxylic group [9,21]. The LAA spectra shows that absence of peak at 2125 cm^{-1} which may be responsible for metal linkage with N of amino group. The peak at 543 cm-1 is ascribed COO^- wagging mode of vibrations [24]. The FT-Raman spectral assignments are shown in Table 3.

4.5. UV–Vis-NIR spectral analysis

Fig. 6, shows the UV–Visible absorption spectra of LAA and LAA + La^{3+} dopant and it reveals 265 nm and 249 nm is their cut off wavelengths respectively [25,26]. There is no absorption in visible region, and it is general for amino acids [37]. Interestingly the doped crystal has reduced absorption and reduced cut-off wavelength. This further showing the dopant improved the transparent property. These properties are improved in the doped crystal rather than pure one is suitable for producing second harmonic generation well [24].

4.6. Micro-hardness studies

Micro-hardness analysis is one among the main study for making components, machine and etc., [27]. Through the Vickers instrument the hardness measurements for both crystals taken from 10 g to 50 g. Fig. 7. shows the hardness vs load along (1 0 0) plane The plot of variations of Vickers hardness number with

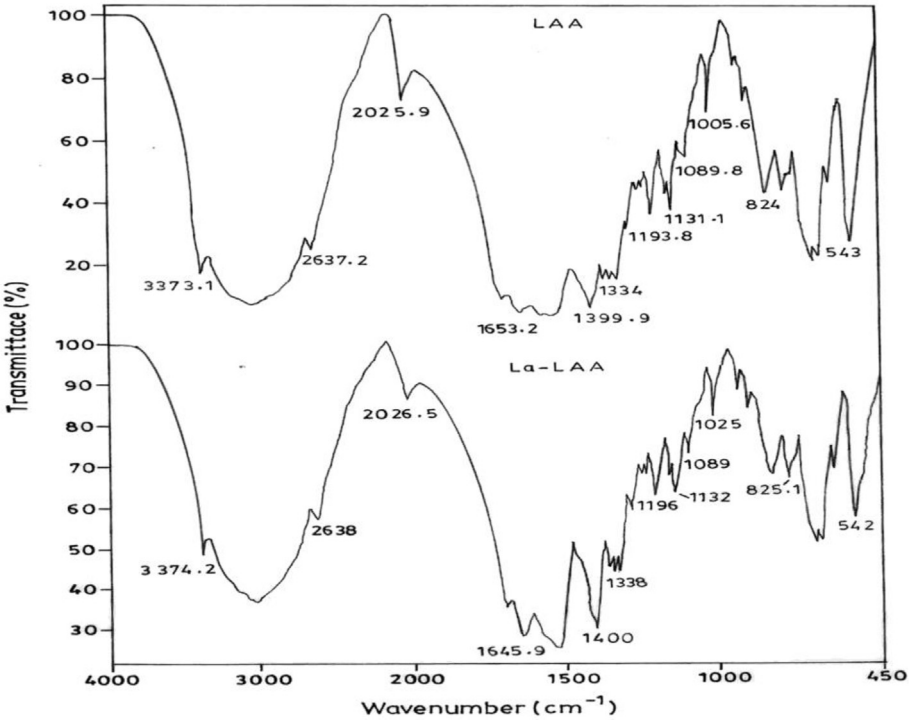

Fig. 4. FT-IR spectrum of pure and La^{3+} doped LAA crystal.

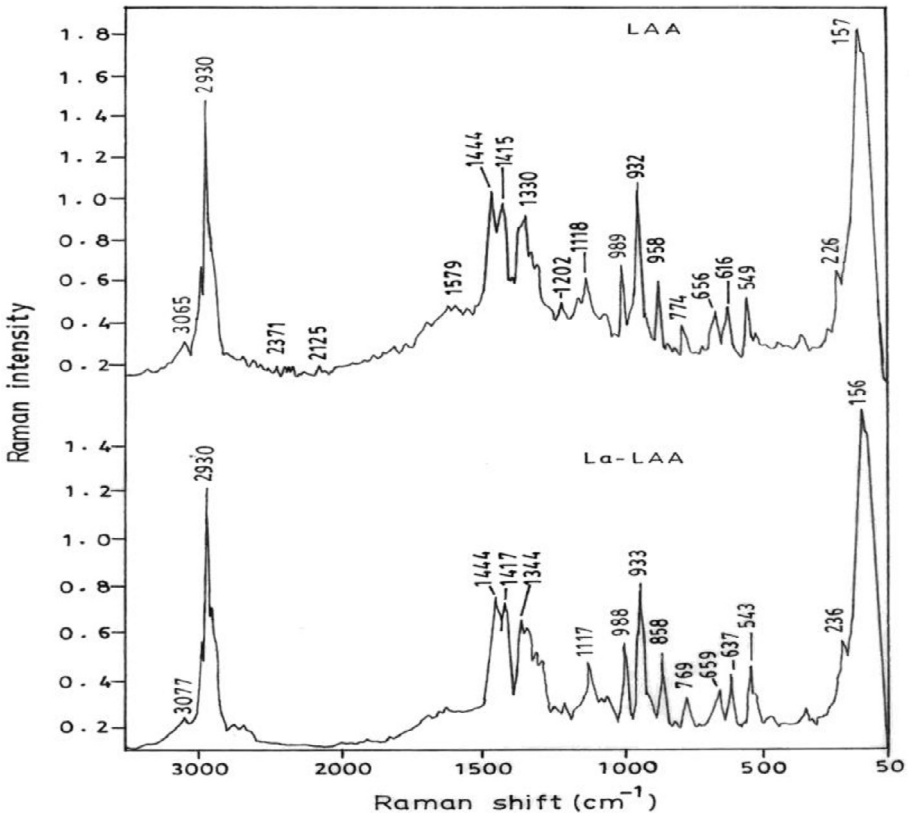

Fig. 5. FT-Raman spectrum of LAA, and La^{3+} + LAA crystal.

Table 3
FT-Raman spectral data of LAA, and La^{3+} + LAA crystal.

Wave number (cm^{-1})		Assignments
Pure LAA	La^{3+}-LAA	
2965	2964	Aliphatic CH_3
2930	2930	Aliphatic CH_2
2125	–	C≡C stretching vibration
1626	1626	Asymmetric C=O stretching
1579	1578	N–H asymmetric deformation
1415	1417	Symmetric C=O stretching
1330	1344	CH_3 symmetric deformation
549	543	COO– wagging mode

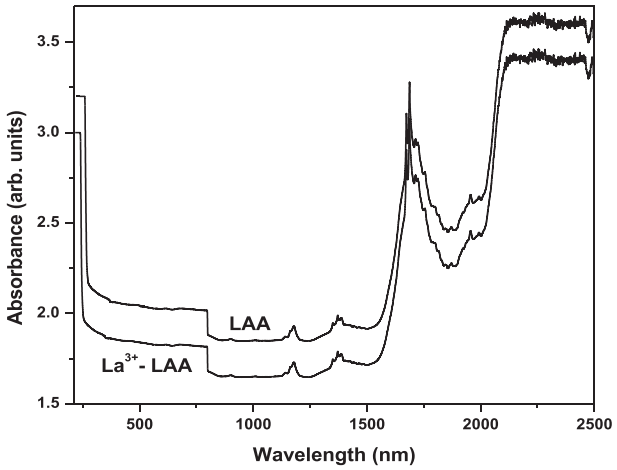

Fig. 6. UV–Visible spectrum of LAA pure and La^{3+} doped LAA crystal.

applied load for (1 0 0) plane. The decrease in hardness from the graph is indicates that decrease in micro hardness with load is agreement well with size effect. After compare both H_V is more in doped crystal [28,29,39].

4.7. Thermal studies

The thermo gravimetric analysis for LAA taken from 23 °C and 1200 °C under N_2 environment heated in steps of 10 K/min. The resulting TG/DTA traces are shown in Fig. 8. Both the pure and doped crystals show two stages of weight loss, 76.42% and 77.92% in the first stage and 23.72% and 19.21% in the second stage for pure and doped crystal respectively [10]. The decomposition starts at 232.9 °C and 228.1 °C respectively for pure and doped samples. The single melting point is the evident for complete crystallinity of crystals [30]. Both the thermogram show negligible

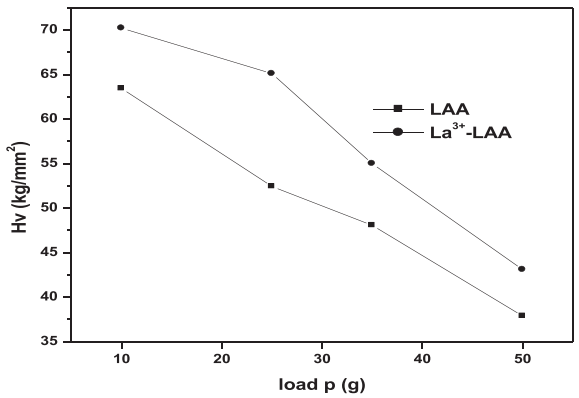

Fig. 7. Hv vs applied load of LAA and LAA + La^{3+} crystal.

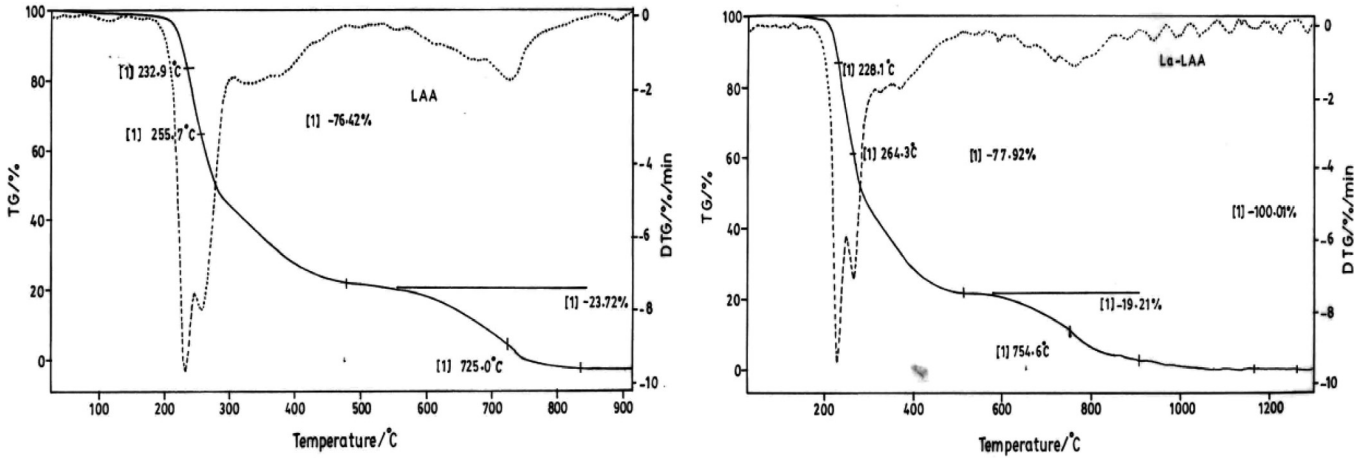

Fig. 8. TGA/DTG curves of LAA, and La^{3+} + LAA crystal.

residue. The decrease in decomposition temperature of the doped crystal is due to the decrease, because of bond energy given by the dopant [24]. The non-existence of addition peaks confirming the absence of water molecules [28].

4.8. NLO studies

The NLO analysis taken for both crystals Kurtz and Perry powder SHG test was carried out on pure and doped LAA single crystals [31]. Nd:YAG laser is the source 1064 nm wavelength, photomultiplier with the reference of Urea crystal [29]. The SHG confirmed green signal of 830 mW, 980 mW and 275 mW were found for LAA, La3+ doped LAA, with reference KDP Crystals respectively. So, the SHG efficiency of LAA crystal is 3.0, LAA + LA^{3+} crystal is 3.6 time than KDEP crystal. And it indicate that La^{3+} dopant enhanced the NLO properties of LAA the pure one [9,32,39]. Further, the enhanced optical NLO properties due to relatively larger in size [33].

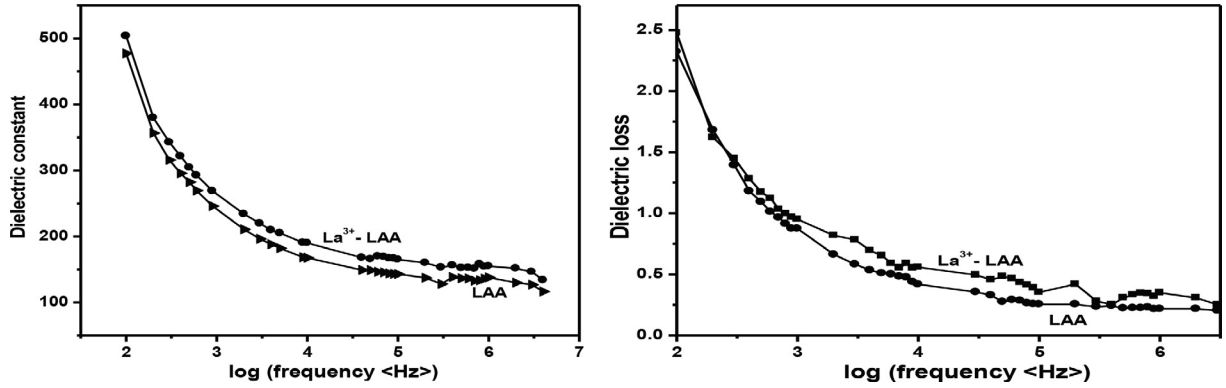

Fig. 9. Dielectric constant, dielectric loss vs LAA and La^{3+} + LAA crystal.

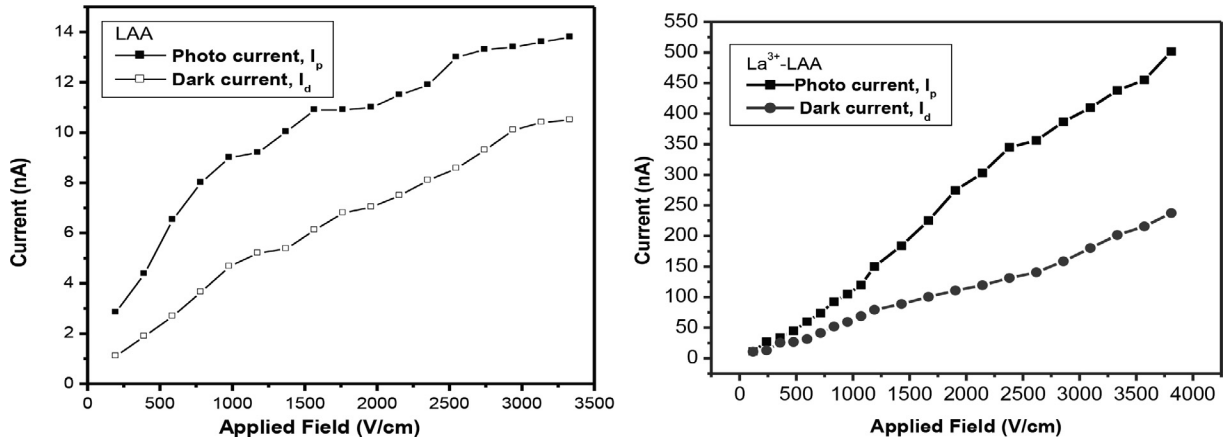

Fig. 10. Photo conductivity and dark conductivity vs applied field of LAA and La^{3+} + LAA crystal.

4.9. Dielectric studies

The capacitance of the crystal was found for the applied frequency that varies from 100 Hz to 5×10^6 at room temperature. Fig. 9 shows the plot of dielectric constant vs. frequency (logarithmic) of both crystals. The dielectric constant is higher in lower region and higher in high frequency region, further the same trend with temperature [32,34]. The space charge polarization depends on purity and the perfectness of the samples. The movement of ion from equilibrium state is due to dipole nature due to charge of ions [34,35]. The dielectric loss and the frequency are completely depends with each other, and the plot of these two are shown in Fig. 10, suggesting their dependency [11]. The low loss in dielectric strongly indicates both crystals have lesser defects. The crystals which exhibiting lower dielectric constant to more region of frequency is need for SHG applications, due to their low dissipation in energy which reflects in efficiency [35,36].

4.10. Photoconductivity studies

The dark current of the sample was measured using DC power supply and picoammeter. The Photo current of the crystals was measured using halogen lamp. DC supply is increased step by step from 10 V to 100 V and the photo current was measured. Fig. 10 shows the photo current and dark current vs field applied for both crystals. It shows that the photocurrent >dark current and so both crystals possess the photoconductive nature, but doped increased enormous [37,38,40].

5. Conclusions

The single crystals of LAA and La^{3+} metal ion doped LAA are grown by slow solvent evaporation process. The monoclinic structure confirmation for both crystals by XRD analysis. The existence of La^{3+} has altered slightly the lattice parameters and there is no change in basic structure of crystals. In the FT-Raman studies of doped LAA, changes are observed in the peak positions, which confirm the presence of dopant in selective site of LAA crystal. The optical transmission spectral analysis shows doped LAA crystals having more optical transparency rather than pure one. The SHG analysis revealed that doped LAA has more NLO properties better than pure LAA crystal. The TG/DTA of pure LAA revealed the decomposition of the sample starts at 262 °C. Both crystal having reasonable hardness resulted from Hv values. The dielectric constant and dielectric loss of the doped samples show marginal changes when compared with pure LAA. The photoconductivity investigations of pure and doped LAA reveal the positive photoconductivity nature.

Declaration of Competing Interest

The authors declare that they have no known competing financial interests or personal relationships that could have appeared to influence the work reported in this paper.

References

[1] B.E.A. Saleh, M.C. Teich, Fundamental of Photonics, Wiley, New York, 1991.
[2] T.R. Moore, R.W. Boyd, Improvement of the photorefractive efficiency of BaTiO3 by γ irradiation, Appl. Phys. Letts. 61 (17) (1992) 2015–2017.
[3] E. Haque, J. Kim, V. Malgras, K. Raghava Reddy, A.C. Ward, J. You, Y. Bando, Md. S.A. Hossain, Y. Yamauchi, Recent advances in graphene quantum dots: synthesis, properties, and applications, Small Methods 2 (1) (2018) 1800050.
[4] V. Navakoteswara Rao, N. Lakshmana Reddy, M. Mamatha Kumari, P. Ravi, M. Sathish, K.M. Kuruvilla, V. Preethi, Kakarla Raghava Reddy, Nagaraj P. Shetti, Tejraj M. Aminabhavi, M.V. Shankar, Photocatalytic recovery of H2 from H2S containing wastewater: Surface and interface control of photo-excitons in Cu2S@ TiO2 core-shell nanostructures, Appl. Catal. B 254 (2019) 174–185.
[5] P. Tanusri, K. Tanusree, Optical, mechanical and thermal studies of nonlinear optical crystal l-arginine acetate, Mater. Chem. Phys. 91 (2005) 343–347.
[6] C.V. Reddy, I.N. Reddy, K.R. Reddy, S. Jaesool, K. Yoo, Template-free synthesis of tetragonal Co-doped ZrO2 nanoparticles for applications in electrochemical energy storage and water treatment, Electrochim. Acta 317 (2019) 416–426.
[7] K.R. Reddy, C.H. Reddy, V. Nadagouda, N. Mallikarjuna, N.P. Shetti, S. Jaesool, T. M. Aminabhavi, Polymeric graphitic carbon nitride (g-C3N4)-based semiconducting nanostructured materials: Synthesis methods, properties and photocatalytic applications, J. Environ. Manage. 238 (2019) 25–40.
[8] N. LakshmanaReddy, V. Navakoteswara Rao, M. Vijayakumar, R. Santhosh, S. Anandan, M. Karthik, M.V. Shankar, Kakarla Raghava Reddy, Nagaraj P. Shetti, M.N. Nadagouda, Tejraj M. Aminabhavi, A review on frontiers in plasmonic nano-photocatalysts for hydrogen production, Int. J. Hydrogen Energy 44 (21) (2019) 10453–10472.
[9] T. Pal, T. Kar, G. Bocelli, L. Rigi, Synthesis, growth, and characterization of L-arginine acetate crystal: a potential NLO material, Cryst. Growth Des. 3 (2003) 13–16.
[10] S.B. Monaco, L.E. Davis, S.P. Velsko, F.T. Wang, D. Eimerl, A. Zalkin, Synthesis and characterization of chemical analogs of L-arginine phosphate, J. Cryst. Growth 85 (1987) 252–255.
[11] R. Muralidharan, R. MohanKumar, R. Jayavel, P. Ramaswamy, Growth and characterization of L-arginine acetate single crystals: a new NLO material, J. Cryst. Growth 259 (2003) 321–325.
[12] M. Gulam Mohamed, M. Vimalan, J.G.M. Jesudurai, J. Madhavan, P. Sagayaraj, Growth and characterization of pure and doped nonlinear optical L-arginine acetate single crystals, Cryst. Res. Technol. 42 (2007) 948–954.
[13] M. Amit, M. Akansha, B. Soumen, S. Nagaraj, R.K. Raghava, A.M. Tejraj, Graphitic carbon nitride (g–C3N4)–based metal-free photocatalysts for water splitting: A review, Carbon 149 (2019) 693–721.
[14] P.L.S. Basavarajappa, B.N.H. Seethya, Nagaraju Ganganagappa, K.B. Eshwaraswamy, R.R. Kakarla, Enhanced photocatalytic activity and biosensing of gadolinium substituted BiFeO3 nanoparticles, ChemistrySelect 3 (31) (2018) 9025–9033.
[15] E. Haque, Y. Yamauchi, V. Malgras, K.R. Reddy, J.W. Yi, Md.S.A. Hossain, J. Kim, Nanoarchitectured graphene-organic frameworks (GOFs): synthetic strategies properties, and applications, chemistry, Asian J. 13 (23) (2018) 3561–3574.
[16] N.P. Shetti, S.D. Bukkitgar, K.R. Reddy, C.V. Reddy, T.M. Aminabhavi, ZnO-based nanostructured electrodes for electrochemical sensors and biosensors in biomedical applications, Biosens. Bioelectron. 141 (2019) 111417.
[17] M.P. Singh, J.B. Baruah, Photophysical properties of phthalimide and pyromellitic diimide tethered imidazolium nitrophenolate salts, Chemistryselect 4 (1) (2019) 10–16.
[18] S.D. Bukkitgar, N.P. Shetti, R.M. Kulkarni, K.R. Reddy, S.S. Shukla, V.S. Saji, T.M. Aminabhavi, Electro-catalytic behavior of Mg-doped ZnO nano-flakes for oxidation of anti-inflammatory drug, J. Electrochem. Soc. 166 (9) (2019) B3072–B3078.
[19] D.B. Shikandar, N.P. Shetti, R.M. Kulkarni, S.D. Kulkarni, Silver-doped titania modified carbon electrode for electrochemical studies of furantril, ECS J. Solid State Sci. Technol. 7 (7) (2018) Q3215–Q3220.
[20] S.D. Bukkitgar, N.P. Shetti, R.M. Kulkarni, S.T. Nandibewoor, Electro-sensing base for mefenamic acid on a 5% barium-doped zinc oxide nanoparticle modified electrode and its analytical application, RSC Adv. 5 (2015) 104891–104899.
[21] K. Meera, R. Muralidharan, R. Dhanasekaran, Prapun Manyam, P. Ramasamy, Growth of nonlinear optical material: L-arginine hydrochloride and its characterisation, J. Crys. Growth 263 (2004) 510–516.
[22] J. Dolinšek, D. Arcon, H.J. Kim, J. Seliger, V. Zagar, P. Vanek, J. Kroupa, Z. Zikmund, J. Petzelt, Two-time clock NMR observation of the ferroelectric transition in the organic compound cyclohexane-1,1′-diacetic acid J, Phys. Rev. B 57 (1998) R8063.
[23] O. Auciello, J.F. Scott, R. Ramesh, The ability of ferroelectric materials to switch robustly from one polarization state to another forms the basis of a new thin film technology for storing data, Phys. Today 51 (7) (1998) 22–27.
[24] K. Ramya, C. Ramachandra Raja, Studies on the growth and characterization of L-arginine maleate dihydrate crystal grown from liquid diffusion, Techn. J. Mine Mat. Charac. Enng. 4 (2016) 143–153.
[25] T. Umadevi, N. Lawrence, B.R. Ramesh, K. Ramamurthy, Growth and characterization of L-prolinium picrate single crystal: A promising NLO crystal, J. Cryst. Growth 310 (2008) 116–123.
[26] J.J. Rodrigues Jr, L. Misoguti, F.D. Nunes, C.R. Mendonça, S.C. Zilio, Optical properties of L-threonine crystals, Opt. Mater. 22 (2003) 235–240.
[27] K.D. Parikh, D.J. Dave, B. Parekh, M.J. Joshi, Thermal, FT–IR and SHG efficiency studies of L-arginine doped KDP crystals, Bull. Mater. Sci. 30 (2) (2007) 105–112.
[28] R. Kanagadurai, R. Sankar, G. Sivanesan, S. Srinivasan, R. Jayavel, Growth and properties of ferroelectric potassium ferrocyanide trihydrate single crystals, Cryst. Res. Technol. 41 (9) (2006) 853–858.
[29] P.V. Radhika, K. Jayakumari, C.K. Mahadevan, Formation and properties of L-arginine acetate single crystals doped with hydrochloric acid, IOSR J. Appl. Phys. 6 (4) (2014) 19–29.
[30] N. Renuka, N. Vijayan, R. Brijesh, R. Ramesh Babu, K. Nagarajan, D. Haranath, G. Bhagavannarayana, Synthesis growth and optical properties of semi organic non linear optical single crystal: l-Arginine acetate, Optik 123 (2012) 189–192.

[31] S.K. Kurtz, T.T. Perry, A powder technique for the evaluation of nonlinear optical materials, J. Appl. Phys. 39 (1968) 3798–3813.
[32] M.A. Pinard, T.A.J. Grell, D. Pettis, M. Mohammed, K. Aslan, Rapid crystallization of L-arginine acetate on engineered surfaces using metal-assisted and microwave-accelerated evaporative crystallization, CrystEngComm 14 (14) (2012) 4557–4561.
[33] S. Aruna, A. Anuradha, P.C. Thomas, M. Gulam, S.A. Rajesekar, M. Vimalan, G. Mani, P. Sagayaraj, Growth optical and thermal studies of L-arginine perchlorate and A promising non-linear optical single crystal, Ind. J. Pure Appl. Phys. 45 (2007) 524–528.
[34] M. Meena, C.K. Mahadevan, Growth and dielectric properties of L-arginine acetate and L-arginine oxalate single crystals, Mater. Lett. 62 (2008) 3742–3744.
[35] P. Vasudevan, S. Sankar, D. Jayaram, electrical studies of nonlinear optical crystal: L-arginine semi-oxalate, Bull. Korean Chem. Soc. 34 (1) (2013) 128–132.
[36] M. Anis, Growth, structural and opto-electrical studies of glycine doped malic acid crystal for nonlinear applications, Res. J. Recent Sci. 3 (9) (2014) 47–51.
[37] R.H. Bube, Photoconductivity of Solids, Wiley, New York, NY, USA, 1981.
[38] K. Rajesh, P. Praveen Kumar, Structural, linear, and nonlinear optical and mechanical properties of new organic L-Serine crystal, J. Materls. (2014) 5, ID 790957.
[39] A. Vijayakumar, A. Ponnuvel, A. Kala, Growth and characterization of pure and doped L-histidine acetate crystals, Mater. Proc. 8 (1) (2019) 484–491.
[40] H.D. Madhuchandra, B.E. Kumara Swamy, Poly (vanillin) modified carbon paste electrode for the determination of adrenaline: A voltammetric study, Mater. Sci. Energy Technol. 2 (2019) 697–702.